

# Quantum Graph-Based Differential Models For Dynamic Analysis Of Protein-Protein Interaction Networks

# Vajjiram Sangeetha<sup>1\*</sup>, K. Kavitha<sup>2</sup>, M. Aruna<sup>3</sup>, R. Ravichandran<sup>4</sup>

#### \*Corresponding Author:

Vajjiram Sangeetha

<sup>1\*</sup>Saveetha School of Engineering, Department of Computational Biology, Kancheepuram (Dt), Tamilnadu, India.

Email ID: sanmatreal@gmail.com

Cite this paper as: Vajjiram Sangeetha, K. Kavitha, M. Aruna, R. Ravichandran, (2025) Quantum Graph-Based Differential Models For Dynamic Analysis Of Protein-Protein Interaction Networks. *Journal of Neonatal Surgery*, 14 (7), 1189-1214.

#### **ABSTRACT**

Understanding Protein-Protein Interaction (PPI) networks is essential for comprehending intricate biological processes, such as disease development and cellular functions. Due to the dynamic and non-linear nature of these connections, modelling and analysing such complex networks is extremely challenging. Existing graph-based frameworks often fail to capture the stochastic behaviour and quantum-level uncertainty inherent in biological structures. This study enhances the dynamic assessment of PPI systems by introducing Quantum Graph-Based Differential Models (QGDM) to overcome these limitations. The proposed method incorporates quantitative transitions between states and probabilistic behaviour in biological systems while modelling time-evolving interactions using inequality equations and classical graph theory concepts. The process involves constructing quantum graphs to represent PPI systems and applying quantum linear equations to describe the structure of interactions. By integrating quantum effects, the model improves predictions of system shifts, leading to a better understanding of biological pathways and system responses. The goal is to provide a more accurate framework for identifying key proteins and predicting the impact of network modifications on functionality. The effectiveness of the proposed model is validated through experimental simulations using real PPI datasets demonstrating enhanced prediction accuracy and resilience compared to traditional methods. The findings indicate a significant improvement in identifying critical nodes and capturing dynamic transitions, paving the way for more effective pharmacological target selection and biomarker development. By addressing key shortcomings of conventional models, this innovative integration of quantum graph concepts and differential modelling offers approach to understanding and analysing biological systems.

**Keywords:** Quantum Graph Theory, Protein-Protein Interaction Networks, Differential Equations, Dynamic Network Analysis, Quantum State Transitions, Biological Network Modeling, Molecular Pathways, System Dynamics, Biomarker Discovery, Drug Target Identification.

#### 1. INTRODUCTION

The term "network" originates from common language used to describe a wide range of well-known and tangible structures. Artificial Neural Networks (ANN) such as roads, railways, air traffic systems, electrical grids, and interpersonal networks; biological systems such as metabolic pathways, blood circulation, and food webs tree-like networks with simpler characteristics such as hydrographic systems [1]. A network consists of a set V of N vertices are connected by a subset E of edges. These edges may have attributes such as weights, orientations, or signs. The network configuration is defined by the set  $(\overline{s}(t)) = [s_i(t); i \in V]$  represents the instantaneous state  $s_i(t)$  of each node i. This state can be either discrete (e.g., a Boolean variable where  $s_i = 1$  or 0) or continuous [2]. A graph is typically represented as G = (V, E), where E is a **Journal of Neonatal Surgery** Year:2025 |Volume:14 |Issue:7

<sup>&</sup>lt;sup>1\*</sup>Saveetha School of Engineering, Department of Computational Biology, Kancheepuram (Dt), Tamilnadu, India.

<sup>&</sup>lt;sup>1</sup>Department of Mathematics, Sun Arts and Science College, Thiruvannamalai, Tamilnadu, India.

<sup>&</sup>lt;sup>2</sup>Department of Mathematics, S. A. Engineering College (Autonomous), Chennai-600077.

<sup>&</sup>lt;sup>3</sup>Department of Mathematics, Immaculate College for Women, Viriyur, Kallakurichi, Tamilnadu India-606402.

<sup>&</sup>lt;sup>4</sup>Centre for Nonlinear Systems, Chennai Institute of Technology, Chennai, Tamilnadu India-600069.

specific subset of  $V \times V$ . If neither (i, j) nor (j, i) belong simultaneously to E, the edges may be oriented even if they are unweighted (i.e., either present or absent). Any pairwise attribute or interaction within a group V of elements can be linked to a network structure: two elements  $i, j \in V$  that share a common property are connected, denoted as  $(i, j) \in E$ . Although this may seem like a simple reformulation of ensemble connections, it proves to be highly valuable. It enables the application of mathematical and geometric principles from graph theory, probabilistic and physics-based methodologies from complex network theory [3].

A graph may or may not be directly connected to a physical space. For instance, the set V can represent discrete points in  $R^3$  (three-dimensional space) or  $R^2$  (a plane) such as road or railway networks [4]. In these cases, the system inherits the spatial separation from the underlying space, assigning each pair (i, j) a distance  $r_{ij}$ . The concept of a graph extends beyond physical connections and includes abstract relationships. V is an arbitrary set of entities that do not inherently possess a linear or topological structure. Examples include social networks within an organization or school, World Wide Web connection strengths have little or no dependence on physical distances [5]. Networks offer a new topological architecture is closely linked to the functional significance of relationships and is often superimposed on an existing topological framework if one exists. The most complex systems arise when the organic structure that evolves over time coexists with the inherent structure of relationships. This interaction influenced by competition, dissatisfaction, or other selection mechanisms can lead to emergent behaviours. Food chains and neural networks are prime examples of such systems where both intrinsic organization and functional connectivity shape their dynamics [6].

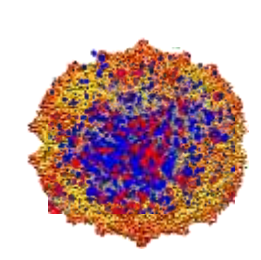
One of the primary objectives of systems biology is to understand both the structure and function of biological systems. In its early stages, biological computation focused on investigating the unique properties of intracellular components and compiling this data into extensive databases. Biological systems are defined by the interactions among their constituent elements [7]. The advent of high-throughput technologies has further enabled the quantitative analysis of these complex structures. Gene networks nodes represent gene products and edges signify molecular interactions provide a framework for analysing biological functions by processing and evaluating high-throughput data [8]. Since multiple approaches exist for deriving networks from high-throughput data, network inference plays a crucial role in network biology. For instance, association networks can be constructed using the WGCNA program, while the minet package can infer relationships based on shared information. Additional methods for network inference using diverse visual representations are available in other packages [9]. Introduced the C3NET methodology and compared it with alternative approaches for identifying the conservative causal core of gene networks. Findings emphasize the importance of accurately constructing reliable and biologically meaningful networks. Structural analysis of biological systems can reveal hidden biological insights that may not be immediately apparent from raw data [10]. A key challenge in network analysis involves identifying topologically significant nodes and characterizing networks based on their organizational structure. To address this, the QuACN R package provides a diverse set of novel topological network descriptors numerically quantify the fundamental properties of a network. Topological network descriptors as measurements, indices, or graph invariants, highlighting their role in objectively describing network structures [11].

The complexity of network quantification has become a significant research challenge across multiple scientific disciplines over the past few decades. In mathematics and medicinal chemistry, particularly in drug design, topological network descriptors such as QSAR/QSPR have been employed to analyse and characterize the physical structures of chemical compounds [12]. In a more biologically driven study, researchers have utilized vertex degrees of PPI networks to correlate organismal and protein structure complexity with the underlying PPI network's intricacy. Their findings indicate a strong correlation between PPI network vertex degrees and PPI domain coverage [13]. Explored the relationship between phylogeny and metabolic network complexity, linking organismal evolution to the arrangement and interactions of metabolic pathways using various network metrics. Their results suggest that phylogenetic distances can be accurately reconstructed using a small subset of network descriptors [14]. A comprehensive discussion of the numerous network metrics developed over time falls beyond the scope of this study. For further insights, an extensive review of network measurements, while offer a compelling summary of existing network descriptors, including information-theoretic metrics. Many aspects regarding the feasibility and characteristics of various descriptors remain unresolved [15].

### 1. Microarray Experiment

# 2. Inferring Networks

# 3. Structural Analysis



$$X_f(G) = -\sum_{x=1}^{|V|} \frac{f(v_x)}{\sum_{y=1}^k f(v_x)} \log \left( \frac{f(v_x)}{\sum_{y=1}^k f(v_x)} \right)$$

# 4. Biological Validation



Figure 1: Structural analysis of microarray network data to biological validation

QuACN offers a diverse range of topological network characteristics, providing a consistent and user-friendly approach to utilizing these indexes. This enables researchers to explore various biological applications using network-based methods [16]. Figure 1 illustrates a typical research framework for the structural analysis of biological systems depicting a generalized procedure for applying network methodologies with topological measurements to analyse microarray technology studies [17]. In general, quantitative network analysis is a complex task, requiring a deep understanding of the methodology to accurately interpret the results. This publication is intended for readers interested in structural network analysis aiming to help them effectively apply the techniques provided by QuACN [18]. This study does not address the challenge of constructing resilient and reliable networks, as it falls beyond its scope. It does not provide a detailed explanation of network metrics or guidance on interpreting topological network descriptor findings [19].

Graphs may be conveniently represented using the adjacency matrix  $A \in R|V| \times |V|$ , which is defined as

$$A[u,v] = A_{uv} = \begin{cases} 1 & \text{if } (u,v) \in \varepsilon \\ 0 & \text{otherwise} \end{cases} (1)$$

In certain situations, it is essential to represent the strength of interactions between nodes. For example, in biology, it can be valuable to indicate how strongly two proteins interact with each other. Adjacency matrix shown in Figure 2 (a) and (b). The adjacency matrix of a weighted graph is defined in Figures 2 (a) – (d). This can be achieved by assigning weights to the edges, as illustrated in Figure 2 (e) and (f). A weighted edge is represented by the triplet( $u, v, w_{uv}$ ), where  $w_{uv} \in \mathbb{R} \setminus \{0\}$  denotes the weight of the edge connecting nodes u and v. In this context, the set of edges E consists of all such triplets ( $u, v, w_{uv}$ ) that define the weighted edges in the graph [20].

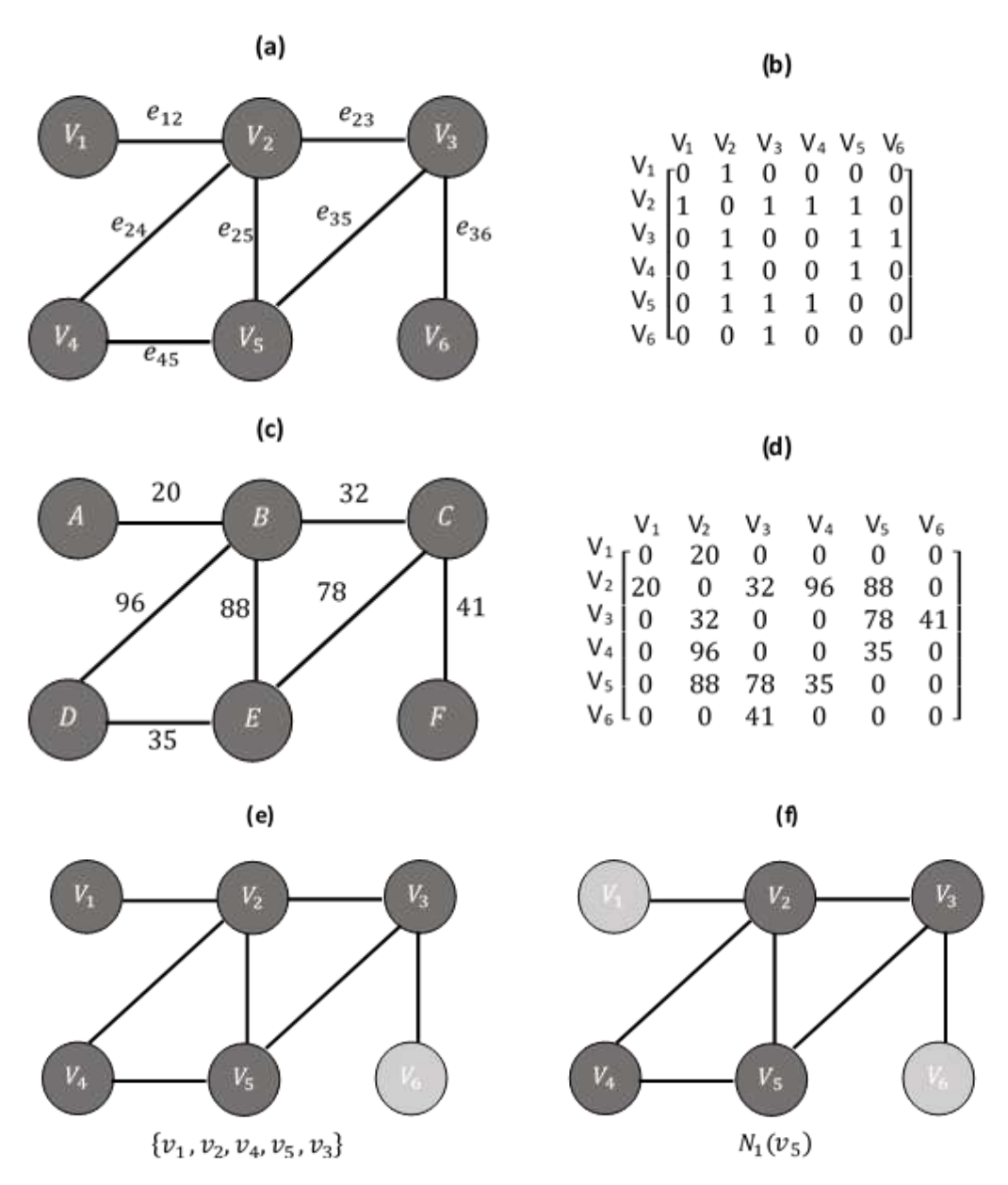


Figure 2: Example Adjacency matrices and its weights (Undirected graphs weighted and unweighted)

$$A[u,v] = A_{uv} = \begin{cases} w_{uv} \ if(u,v,w_{uv}) \in \varepsilon \\ 0 \ otherwise \end{cases} \tag{2}$$

#### 2. GRAPH PROPERTIES

PPI networks with other complex networks such as biological systems, rely significantly on graph-based features. The adjacency matrix (A) represents the structural connections within the graph, while the degree of a vertex d(v) quantifies the number of edges incident to that vertex. Graph connectivity is assessed using the Laplacian matrix (L) is derived from both the degree and adjacency matrices. The spectral radius  $(\rho)$  calculated from the eigenvalues of the adjacency or Laplacian matrix provides insight into the network stability. The clustering coefficient C(v) measures the likelihood that a vertex's neighbors form triangular connections. Betweenness centrality B(v) highlights critical nodes that frequently appear on shortest paths, while the average path length (L) evaluates the efficiency of information flow across the network. The graph diameter  $d_{max}$  indicates the length of the longest shortest path between any two nodes whereas graph density (D) reflects the overall level of connectivity within the network. Finally, graph entropy (H(G)) captures the complexity and structural information of the network. Collectively, these graph characteristics provide a comprehensive framework for analysing and understanding the architecture and behaviour of dynamic and biological systems.

**Definition 2.1: Degree d(v) -** The degree of a vertex is the number of edges connected to it. In undirected graphs, it counts the number of neighbors.

$$d(v) = \sum_{u \in N(v)} 1$$
 (3)

Where N(v) is the set of neighbors of vertex v.

**Definition 2.2:** Adjacency Matrix (A) Square matrix of size  $n \times n$ , where n is the number of vertices. It records the presence or absence of edges between nodes.

$$A_{xy} = \begin{cases} 1 & if(v_x, v_y) \in \varepsilon \\ 0 & otherwise \end{cases}$$
 (4)

Where E is the set of edges.

**Definition 2.3: Laplacian Matrix (L)** It is used to represent the structural properties of a graph and is calculated as the difference between the degree matrix (D) and the adjacency matrix (A),

$$L = D - A (5)$$

Where: D is the degree matrix (diagonal matrix where  $D_{xx} = d(v_x)$ ). A is the adjacency matrix

**Definition 2.4: Eigenvalues and Spectral Radius** The eigenvalues of the adjacency or Laplacian matrix offer valuable insights into key graph properties, such as connectivity and stability.

Spectral Radius ( $\rho$ ):  $\rho(G) = max\{|\lambda_x|: \lambda_x \text{ is an eigenvalue of } A\}$  (6)

**Definition 2.5:** Clustering Coefficient (C(v)) The clustering coefficient of a vertex quantifies the likelihood that its neighbors form a complete subgraph, such as a triangle.

$$C(v) = \frac{2T(v)}{d(v)(d(v)-1)}$$
 (7)

Where T(v) the number of triangles passing through vertex v.

**Definition 2.6: Average Path Length (L)** Length between all pairs of nodes measures the efficiency of information flow in the network.

$$L = \frac{1}{n(n-1)} \sum_{x \neq y} d(v_x, v_y)$$
(8)

Where  $d(v_x, v_y)$  is the shortest distance between vertices  $v_x$  and  $v_y$ 

**Definition 2.7: Betweenness Centrality (B(v))** Centrality measures the importance of a node by quantifying the proportion of shortest paths that pass through it.

$$B(v) = \sum_{s \neq v \neq t} \frac{\sigma_{st}(v)}{\sigma_{st}}$$
(9)

Where:  $\sigma_{st}$  is the total number of shortest paths between s and t.

 $\sigma_{st}(v)$  is the number of those paths passing through v.

Definition 2.8: Graph Density (D) quantifies how densely the edges are distributed in the graph.

$$D = \frac{2|E|}{n(n-1)} \quad (10)$$

Where: |E| is the number of edges. n is the number of vertices.

**Definition 2.9: Graph Diameter**  $(d_{max})$  Centrality indicates a node's significance by measuring how often it lies on the shortest paths between other nodes.

$$d_{max} = \max_{x,y \in V} d(v_x, v_y)$$
(11)

Where  $d(v_x, v_y)$  is the shortest distance between vertices  $v_x$  and  $v_y$ 

**Definition 2.10: Graph Entropy (H(G)) quantifies** a graph's structural complexity and the amount of information it contains.

$$H(G) = -\sum_{v \in V} p(v) \log p(v)$$
 (12)

Where:  $p(v) = \frac{d(v)}{2|E|}$  representing the probability of selecting an edge attached to vertex v.

These properties are crucial for analysing the structure, dynamics, and functional behaviour of complex biological and PPI networks.

# 3. THEORETICAL FOUNDATIONS FOR QUANTUM GRAPH-BASED DIFFERENTIAL MODELS IN PPI NETWORKS

The proposed Quantum Graph-Based Differential Models for PPI systems present a unique structure for analyzing dynamic biological relationships by utilizing equations of motion and quantum graph theory concepts. Antibodies and their relationships appear as nodes and edges, accordingly, in the method's quantum graph representation of the PPI system. A quantum state transition theory accurately forecasts modifications to networks by capturing time-evolving connections utilizing Schrödinger-like equations. The quantum graph Laplacian is used to examine the stability of these transitions, and eigenvalues reveal information about the resilience of the system. Furthermore, probability node influence identifies possible targets for drug development by quantifying the effect of perturbation on important nodes. By improving our knowledge of molecular processes, this integrated strategy guarantees more accurate forecasts and effective discovery of important proteins in intricate systems of biology.

# 3.1 Line Graph of Cycle graph $(C_n)$

A cycle graph  $C_n$  is a simple graph of order n (where  $n \ge 3$ ) with exactly n edges. Each edge forms a cycle of length n, and every vertex in the graph has a degree of two. The line graph of a cycle graph, denoted as L(G) is isomorphic to the original cycle graph G. In this line graph, the number of vertices remains the same, and two vertices in L(G) are adjacent if and only if their corresponding edges in G share a common vertex.

**Theorem 3.1.1.** If G is a simple, connected cycle graph  $C_n$  with n vertices, then the line graph L(G) is also a cycle graph with n vertices.

i) 
$$2 \le \gamma_f(G) + \gamma_f(L(G)) \le \frac{2n}{3}$$
 (13)

ii) 
$$1 \le \gamma_f(G) * \gamma_f(L(G)) \le \frac{n^2}{9}$$
 (14)

iii) 
$$\Gamma_f(G) + \Gamma_f(L(G)) = n$$
 (15)

iv) 
$$\Gamma_f(G) * \Gamma_f(L(G)) = \frac{n^2}{4}$$
 (16)

Proof: i) and ii) with the reference of previous chapter for cycle graph we have fractional domination number is  $\gamma_f(C_n) = \frac{n}{3}$  where n = 3, 4, 5... The line graph of cycle graph is L(G) isomorphic to its cycle graph G with same vertex numbers and are adjacent in the provided graph if the corresponding edges share a common vertex. Therefore, for line graph L(G) the fractional dominating number is  $\gamma_f(L(C_n)) = \frac{n}{3}$  For the sum  $\gamma_f(G) + \gamma_f(L(G))$  lower bound is 2 and upper bound is  $\frac{2n}{3}$ . Therefore we have

# **Proof:**

i) Established that for a cycle graph  $C_n$  the fractional domination number is

$$\gamma_f(C_n) = \frac{n}{3}$$
, where n=3,4,5,... (17)

ii) The line graph of a cycle graph, denoted L(G), is isomorphic to the original cycle graph G. This is because each edge in  $C_n$  shares a common vertex with exactly two other edges, and in L(G), these edges become vertices connected by adjacency if their corresponding edges in G share a vertex. Therefore,  $L(C_n) \cong C_n$ 

Hence, the fractional domination number of the line graph is also:

$$\gamma_f(L(C_n)) = \frac{n}{3}$$
 (18)

For the sum of fractional domination numbers, get:

$$\gamma_f(G) + \gamma_f(L(G)) = \frac{n}{3} + \frac{n}{3} = \frac{2n}{3}$$
 (19)

Since  $n \ge 3$ , we have:

Following bounds for the fractional domination number of a cycle graph  $G=C_n$  and its line graph L(G):

$$2 \leq \gamma_f(G) + \gamma_f(L(G)) \leq \frac{2n}{3}$$

$$1 \le \gamma_f(G) * \gamma_f(L(G)) \le \frac{n^2}{9}$$
, Where  $n = 3,4,5,...$ 

Thus, the lower bound for the sum is 2, and the upper bound is  $\frac{2n}{3}$ 

iii) and iv) The upper fractional domination number of the cycle graph  $\mathcal{C}_n$  is:

$$\Gamma_f(C_n) = \frac{n}{2}(20)$$

This is observed by assigning a weight of  $(\frac{1}{2})$  to every vertex. The condition for the upper fractional domination number requires that for every vertex  $w \in V$ , there exists a vertex  $w \in N[v]$  such that:

$$\sum_{v \in N[w]} f(v) = 1$$
 (21)

This condition is satisfied under the weight assignment mentioned above.

Since  $L(C_n) \cong C_n$  we also have:

$$\Gamma_f(G) + \Gamma_f(L(G)) = n$$

$$\Gamma_f(G) * \Gamma_f(L(G)) = \frac{n^2}{4}$$

Theorem 3.1.2: Let G be an r-regular graph of order n. Then, the upper fractional domination number of G satisfies

$$\Gamma_f(G) \leq \frac{n}{r}$$

#### Proof

If G is an r-regular graph of order n, then its fractional domination number satisfies

$$\gamma_f(G) \le \frac{n}{r+1}$$

This is achieved by assigning a weight of  $\frac{1}{r+1}$  to each vertex in G results in a valid fractional dominating function f of minimal total weight.

Similarly, for the upper fractional domination number  $\Gamma_f(G)$ , we consider a function f that assigns a weight of  $\frac{1}{r}$  to each vertex. This function yields the maximum total weight under the fractional domination condition:

$$\sum_{v \in N[v]} f(v) \ge 1 \text{ for all } w \in V(G)$$

Hence  $\Gamma_f(G)$  is defined as

 $\Gamma_f(G) = \max\{|f| \text{ is minimal fractional dominating function of } G\}.$ 

Therefore, for an r-regular graph of order n, the upper fractional domination number satisfies:

$$\Gamma_f(G) \leq \frac{n}{r}$$
.

#### Theorem 3.1.3: Unitary Evolution of Quantum States in a Connected PPI Network

Let G = (V, E) be a connected PPI network represented as a quantum graph, and let the system's state at time t be given by the quantum state vector  $\Psi(t)$  evolving under the Schrödinger equation

$$x\hbar \frac{\partial \Psi(t)}{\partial t} = H\Psi(t)$$
 (22)

with Hamiltonian  $H = -\gamma L$  where L is the Laplacian matrix of G and  $\gamma > 0$  is a scaling parameter). Then the evolution operator

$$U(t) = e^{-xxHt/\hbar} (23)$$

is unitary i.e,

$$U(t)^{\dagger}U(t) = X(24)$$

which guarantees that the total probability is preserved over time.

# **Proof:**

1. By definition, the evolution operator is given by

$$U(t) = e^{-xxHt/\hbar} (25)$$

2. Since the Hamiltonian H is a Hermitian operator (which follows because L is symmetric for an undirected network and  $\gamma$  is real), we have:

$$H = H^{\dagger}$$
 (26)

3. It is a standard result in linear algebra that if H is Hermitian, then U(t) is unitary. To show this explicitly:

$$U(t)^{\dagger} = (e^{-xHt/\hbar})^{\dagger} = e^{xHt/\hbar}$$
 (27)

and thus,

$$U(t)^{\dagger} = (e^{-xHt/\hbar})^{\dagger} = e^{xHt/\hbar}$$
 (28)

4. Since U(t) is unitary, the norm of  $\Psi(t)$  is preserved:

$$||\Psi(t)||^2 = ||U(t)\Psi(0)||^2 = ||\Psi(0)||^2$$
 (29)

Thus, the evolution is unitary and preserves probability.

# 3.2 Lemma: Zero Eigenvalue of the Laplacian for a Connected Graph

#### **Statement:**

Let G = (V, E) be a connected graph. Then the Laplacian matrix L = D - A has exactly one eigenvalue equal to zero, and the corresponding eigenvector is the constant vector 1 (up to normalization).

#### **Proof:**

The Laplacian L is defined as 
$$L_{xy} = \begin{cases} d_x, & \text{if } x = y, \\ -1, & \text{if } x \neq y \text{ and } (x, y) \in E \\ 0, & \text{otherwise} \end{cases}$$
 (30)

Where  $d_x = \sum_y A_{xy}$  is the degree of node x.

Consider the vector  $1 = [1, 1, ..., 1]^T$ . For each component,

$$(L1)_x = d_x - \sum_{y:(x,y)\in E} 1 = d_x - d_x = 0$$
 (31)

Hence, L1 = 0, means that 0 is an eigenvalue with eigenvector 1.

For a connected graph, it is a well-known property that the zero eigenvalue is unique.

# 3.3 Case Study: A Simple 3-Node PPI Network

Consider a small PPI network with 3 proteins. Let the adjacency matrix be

$$A = \begin{bmatrix} 0 & 1 & 1 \\ 1 & 0 & 1 \\ 1 & 1 & 0 \end{bmatrix}$$

The degree matrix is:

$$D = \begin{bmatrix} 2 & 0 & 0 \\ 0 & 2 & 0 \\ 0 & 0 & 2 \end{bmatrix}$$

Thus, the Laplacian matrix is:

$$L = D - A = \begin{bmatrix} 2 & -1 & -1 \\ -1 & 2 & -1 \\ -1 & -1 & 2 \end{bmatrix}$$

#### **Eigenvalue Decomposition**

For this L, the eigenvalues can be computed to be:  $\lambda_1 = 0$ ,  $\lambda_2 = 3$ ,  $\lambda_3 = 3$ .

The eigenvector corresponding to  $l\lambda_1 = 0$  proportional to  $1 = [1, 1, 1]^T$  confirming our lemma.

# **Quantum State Evolution**

Assume the Hamiltonian is defined as:  $H = -\gamma L$ 

with 
$$\gamma = 1$$
 (and setting  $\hbar = 1$  for simplicity). Then,  $H = -\begin{bmatrix} 2 & -1 & -1 \\ -1 & 2 & -1 \\ -1 & -1 & 2 \end{bmatrix}$ 

If the initial quantum state is uniformly distributed,  $\psi(0) = \frac{1}{\sqrt{3}} \begin{bmatrix} 1 \\ 1 \\ 1 \end{bmatrix}$ 

the state at time t is given by:  $\psi(t) = e^{-xHt}\psi(0)$ 

Using the spectral decomposition of H as:  $\psi(t) = \sum_{\nu=1}^{3} e^{-x\lambda t} \langle v_{\nu} | \psi(0) \rangle v_{\nu}$ 

where  $\lambda_1 = 0$  (with eigenvector  $v_1 \infty [1,1,1]^T$  and  $\lambda_2 = \lambda_3 = -3$ . This shows that the network evolves according to the contributions from each Eigen mode and the unitary evolution guarantees that  $||\psi(t)||^2 = 1$  for all t.

This simple example demonstrates how the quantum state evolves over time in a PPI network using our defined Hamiltonian and confirms the theoretical properties stated in the theorem and lemma. Such an approach can be extended to larger PPI networks, allowing for dynamic analysis of protein interactions in a probabilistic and quantum-mechanical framework. This complete example-featuring a theorem with proof, a lemma, and a case study-illustrates the fundamental principles underlying QGDM for dynamic analysis of PPI networks.

#### 3.4 Graphs to model systems

PPI, metabolic networks, and Gene Regulatory Networks (GRNs) are the three primary biological frameworks commonly used to characterize organisms. Drug-Drug Interaction (DDI) networks are included in this category due to their growing significance in modern healthcare research.

# 3.4.1 PPI networks

PPI networks represent the interactions between proteins. All cellular activities including transcription, translation, active transport, cytoskeleton formation, and the development of other structural components depend on these interactions. PPIs also include transient interactions, where protein complexes are easily formed and disassembled. In PPI networks, proteins are represented as nodes, while edges denote the interactions between connected proteins. A comprehensive graphical representation of PPIs would ideally include the type of interaction such as phosphorylation or binding but in practice, such detailed information is rarely documented.

#### 3.4.2 Gene Regulatory Networks

Gene Regulatory Networks (GRNs) represent the intricate mechanisms that control gene expression and the sequence of events leading to protein production from DNA. Regulation occurs at multiple stages of protein synthesis, including transcription, translation, and splicing. These regulatory processes are complex and interconnected. From an intuitive perspective, regulators are both the cause and the consequence of gene expression, highlighting the dynamic and reciprocal nature of gene regulation.

### 3.4.3 Metabolic networks

Metabolic systems are commonly represented using graphs to illustrate metabolism, which comprises all the chemical reactions that occur within a living organism to maintain life. The metabolites are the intermediate and final products of these processes are known as metabolic components. Due to the complexity of these systems, metabolism is typically divided into metabolic pathways specific sets of chemical reactions dedicated to particular biological functions. In this graphical representation, nodes correspond to metabolites, while directed edges represent biochemical reactions, each annotated with the enzyme that facilitates the reaction

#### 3.4.4 Drug-drug interaction networks

Drug—drug interaction (DDI) networks are designed to model the relationships between various pharmaceuticals. In these networks, drugs are represented as nodes, and edges indicate interactions between them. Unlike the previously mentioned networks, a DDI network does not illustrate a biological process directly. These examples highlight the effectiveness of graphs in modelling complex biological information. When utilizing such graphs, it's important to recognize their potential biases and limitations. For instance, research biases can lead to the underrepresentation of specific proteins, genes, or drugs. This often occurs because some biological entities are more costly or difficult to study, prompting researchers to focus on previously explored proteins, genes, or drugs. As a result, proteins with higher degrees in the network may appear to be more important than they truly are, simply because they have been studied more extensively. Certain types of interactions may be underrepresented because they are more difficult to detect or validate. Experimental noise may also be introduced through wet-lab experiments or computational predictions, which sometimes report false positives. One way to mitigate this is by considering interactions supported by multiple sources. For example, databases like STRING assign a confidence score to interactions, indicating the likelihood that the reported interaction is biologically meaningful. A protein's primary structure is composed of a sequence of amino acids that folds into a three-dimensional shape, enabling it to perform essential biological functions. This 3D structure is often represented using contact maps, which are matrices indicating the pairwise physical distances between amino acids. These contact maps can be readily converted into graph

representations, where nodes represent individual amino acids, and edges denote spatial proximity within a specified distance threshold. An example of this transformation for a specific protein is illustrated in Figure 3.

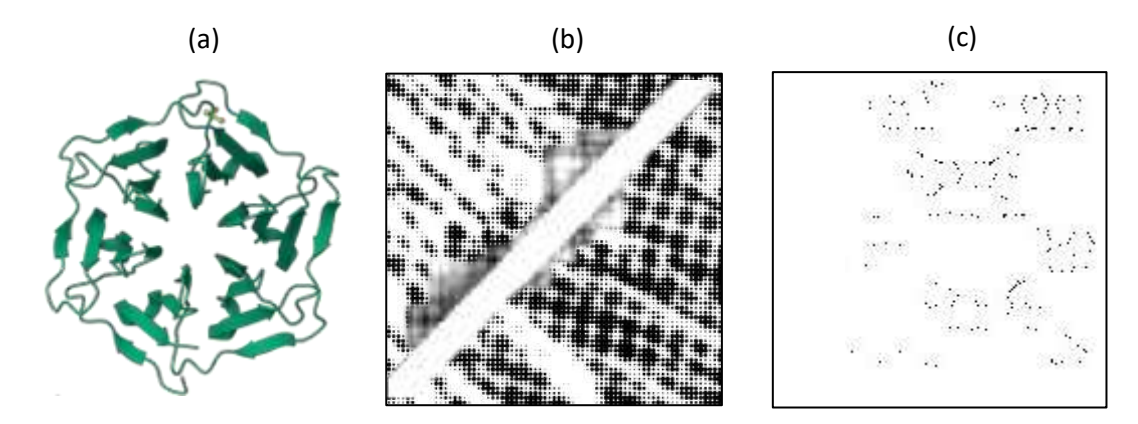


Figure 3 (a) 3D structure of PPI (b) ConPlot map generated by PPI (c) Contact map obtained by adjacency matrix

# 3.5 Dataset description

The data set used for the research includes several features that characterize a PPI system. A Protein ID is assigned to each protein content, making identifying and cross-referencing easier. The dataset contains Interaction Pairs compose the network's edges and indicate links between two proteins (i, j). Every pair of interactions is given an Interaction Score, which ranges from 0 to 1 and reflects the interactions' degree of certainty. While the Gene Name helps with the research of gene-protein relationships by connecting the protein's sequence to its encoding gene, the Biological Role explains how the proteins participate in different aspects of biology. While subcellular location identifies the cellular compartments in which the protein of interest is predominantly found, Pathway Data offers details on the biological processes in which the molecule is engaged shown in Table 1. The degree indicates the number of direct contacts (edges) that are associated with an individual protein, suggesting its position of importance within the structure, while the edge weight indicates the intensity or significance of the link between two proteins. Accurate estimation and evaluation of dynamic PPI systems are made possible by this extensive database.

Attribute Description Data Type Protein ID Unique identifier for each protein String Interaction Pair Tuple Pair of interacting proteins (i, j) Interaction Score Float Confidence score of interaction (range: 0 to 1) **Biological Role** Functional annotation describing the role of the protein String Gene Name Name of the gene encoding the protein String Experimental Evidence Indicates whether the interaction is experimentally validated Boolean Pathway Information Pathway where the protein is involved String Subcellular Location Cellular compartment where the protein is located String Edge Weight The weight assigned to the interaction for network analysis Float Degree Number of direct interactions a protein has Integer

**Table 1: Dataset Description** 

Tuble 21 Sumple David									
Protein ID	Gene Name	Interaction Pair (i, j)	Interaction Score	Biological Role	Experimental Evidence	Pathway Information	Subcellular Location	Edge Weight	Degree
P12345	TP53	(P12345, Q67890)	0.95	Tumor Suppressor	Yes	Apoptosis Pathway	Nucleus	0.85	12
Q67890	MDM2	(Q67890, P12345)	0.92	Oncogene	Yes	p53 Signaling Pathway	Cytoplasm	0.80	8
A45678	BRCA1	(A45678, B34567)	0.88	DNA Repair	Yes	Homologous Recombination	Nucleus	0.78	10
B34567	RAD51	(B34567, A45678)	0.90	DNA Repair	Yes	DNA Repair Pathway	Nucleus	0.82	9
C98765	AKT1	(C98765, D12345)	0.89	Cell Survival	No	PI3K/AKT Signaling	Cytoplasm	0.76	7
D12345	PTEN	(D12345, C98765)	0.87	Tumor Suppressor	Yes	PI3K/AKT Signaling	Cytoplasm	0.74	6

Table 2: Sample Data

To facilitate dynamic network representation and assessment, this sample highlights the biological relevance, pattern of interactions, and confidence ratings of protein pairings, illuminating the PPI dataset's salient features shown in Table 2.

#### 3.6 Spectral Analysis using Laplacian Matrix and Random Walks

By integrating principles from graph theory and quantum physics, quantum graph-based differentiation simulations provide a sophisticated framework for analysing the dynamic evolution of PPI systems. A PPI system can be represented as an undirected graph G=(V,E), where the nodes V represent proteins and the edges E represent interactions between them. The evolution of the quantum state vector  $\Psi(t)$  describes the state of the network at any given time t governed by a Schrödinger-like equation that models the probabilistic changes in protein states. Dynamic analysis plays a crucial role in understanding the functional progression and time-dependent alterations in proteins within PPI networks (PPINs). These dynamic fluctuations are effectively captured using differentiated quantum graph frameworks incorporate quantum mechanical behavior into traditional graph-theoretical models.

# 3.6.1 Quantum Graph Dynamics

To simulate quantum dynamics on a graph, quantum states are assigned to its vertices. Let  $\psi(t)$  denote the quantum state of the system at time t, where  $\psi(t)$  is a vector residing in the Hilbert space linked to the graph. The evolution of this quantum state follows the Schrödinger equation:

$$x \frac{d}{dt} \psi(t) = H \psi(t)$$
 (32)

Where H - Hamiltonian operator that governs the evolution of the system. Quantum graph model chosen as:

$$H = -\gamma L$$
 (33)

Where,  $\gamma$  is a constant related to the strength of interactions. This operator models the dynamics of protein interactions in the network

#### 3.6.2 Spectral Analysis of the Laplacian

The spectral characteristics of the Laplacian matrix offer valuable insights into the structure and dynamic behavior of PPINs. The eigenvalues  $\lambda_x$  and corresponding eigenvectors  $v_x$  of the Laplacian matrix L are obtained by solving the following eigenvalue problem:

$$Lv_x = \lambda_x v_x$$
 (34)

Where  $\lambda_x$  are the eigenvalues and  $v_x$  are the corresponding eigenvectors. These eigenvalues reflect the connectivity and flow of information across the network. Smaller eigenvalues indicate highly connected nodes, while larger eigenvalues suggest less connectivity.

The spectral decomposition of the Laplacian matrix L is given by:

$$L = \sum_{x} \lambda_{x} v_{x} v_{x}^{T}$$
 (35)

Where  $\lambda_x$  are the eigenvalues and  $v_x$  are the eigenvectors.

# 3.6.3 Random Walk on the Graph

To incorporate the concept of diffusion and information propagation across the network, we analyse random walks on the graph. The random walk transition matrix P for a graph is related to the normalized Laplacian tilde  $\bar{L}$  defined as:

$$\bar{L} = D^{-1/2}LD^{-1/2}$$
 (36)

where  $D^{-1/2}$  the inverse square root of the degree matrix. The random walk transition probability is then given by:  $P = X - \bar{L}$  (37)

The random walk process on the graph models how information (such as protein interactions) diffuses through the network over time.

#### 3.6.4 Dynamic Quantum Walk

For a more advanced analysis, consider the dynamic evolution of quantum walks on the graph. This can be modelled using the time-dependent Schrödinger equation for a quantum walk on a graph, where the Hamiltonian is modified to include time-dependent factors. The evolution equation becomes:

$$x \frac{d}{dt} \psi(t) = H(t) \psi(t)$$
(38)

Where H(t) incorporates dynamic interactions, such as changes in protein activity or environmental factors affecting the network.

# 3.6.5 Derivation of Quantum Graph Dynamics

To derive the quantum graph model, we start by discretizing the Schrödinger equation on the graph:

$$x \frac{d}{dt} \psi(t) = -\gamma \sum_{y} L_{xy} \psi_{y}(t)$$
 (39)

Equation (39) describes how the quantum state at each vertex x evolves based on the interactions (edges) with other vertices y. The Laplacian matrix elements  $L_{xy}$  define the interaction strength between vertices x and y. Output is shown in Equation (40).

$$\psi(t) = e^{-x_{\gamma}Lt}\psi(0) \quad (40)$$

where  $\psi(0)$  the initial quantum state at time t = 0

The QGDM provides a powerful framework for analysing dynamic protein-protein interactions in networks. The combination of spectral analysis, random walks, and quantum dynamics offers a comprehensive view of how protein interactions evolve over time, allowing for deeper insights into their functional roles in cellular processes.

#### 3.7 Implementation

Everyone put into practice a few of the topological networking descriptors refer to the package vignette or other literature for a thorough explanation of every descriptor that has been incorporated in QGDM. The following groupings might be used to group the measures:

# Descriptors based on distances in a graph

This category comprises metrics that quantify the structural complexity of a system based on the distances between its nodes. A well-known and classic example is the Wiener index calculated by summing the shortest path distances between all pairs of nodes in the network.

#### Descriptors based on other graph invariants

The adjacency matrix and vertex count are used to compute the normalized edge complexity. An overview of the topology network characteristics that have been implemented in the Table 3.

Table 3: Topology networks used in QGDM

Descriptor	Mathematical Representation	Applications
Degree Distribution	$P(k) = \frac{N_k}{N} (41)$	Analysis of node importance and network resilience
Clustering Coefficient	$C_x = \frac{2e_x}{k_x(k_x - 1)} \tag{42}$	Understanding local network cohesion and motifs
Shortest Path Length	d(u, v)	Network efficiency, communication delay analysis
Average Path Length	$\langle L \rangle = \frac{1}{N(N-1)} \sum_{xy \in V} d(x, y) $ (43)	Global network efficiency, communication cost
Degree Centrality	$C_D(x) = \frac{k_X}{(N-1)}$ (44)	Identifying influential nodes, network hubs
Eigenvector Centrality	$C_E(x) = \frac{1}{\lambda} \sum_{y} A_{xy} C_E(y)  (45)$	Identifying nodes with the highest global influence
Assortativity	$r = \frac{\sum_{xy} A_{xy} k_x k_y}{\sum_{xy} k_x k_y} \tag{46}$	Understanding degree correlation in networks (eg, social networks)
Modularity	$Q = \frac{1}{2m} \sum_{xy} \left( A_{xy} - \frac{k_x k_y}{2m} \right) \delta(c_x, c_y)$ (47)	Community detection in networks
Rich-Club Coefficient	$\phi(k) = \frac{N_k}{N} $ (48)	Identifying core groupings in the network
Local Efficiency	$E_{x} = \frac{1}{k_{x}(k_{x}-1)} \sum_{y,l \in N(x)} \frac{1}{d(y,l)} $ (49)	Understanding the robustness and local efficiency of the network

Note:  $N_k$  – number of nodes with degree k; N - total number of nodes;  $e_x$  - number of edges between the neighbors of node x;  $k_x$  – degree of node x; A - adjacency matrix;  $\lambda$  - largest eigenvalue of the matrix;  $k_x$  and  $k_y$  - degrees of nodes x and y;  $A_{xy}$  is the adjacency matrix; m - number of edges;  $\delta$  is the Kronecker delta function ;

To analyse the dynamics and structure of complex networks such as PPINs, topological network descriptors are essential. These descriptors capture various aspects of connectivity, node importance, and overall network architecture. For instance, a node with a high degree may represent a protein involved in numerous interactions, indicating its potential importance. The clustering coefficient reflects the local cohesiveness of the network and helps understand how proteins with similar functions tend to cluster together.

Betweenness centrality identifies nodes that act as bridges, facilitating communication between distant parts of the network. Eigenvector centrality highlights nodes that are connected to other important nodes signifying their overall influence within the network. Modularity measures the extent to which a network can be divided into communities or

functional clusters, offering insights into the organization of protein groups. Coefficient assesses whether high-degree nodes tend to be more interconnected, revealing a potential "core" of influential proteins. Local efficiency evaluates how effectively information is transferred within a node's immediate neighbourhood is critical for understanding localized processes within the broader system. These descriptors provide a comprehensive understanding of the underlying biological mechanisms, help identify key proteins, and reveal the structural characteristics of the PPIN.

#### 3.8 Linear Programing Problem Formulation of the Graph

Let G = (V, E) be an undirected graph with V is set of vertices and E is set of edges. Decision variable  $f(v) = i_v$  binary decision variable indicating whether vertex v is dominated.

 $f(v) = i_v = 1$  if vertex v is dominated and  $(v) = i_v = 0$  otherwise.

**3.8.1 Objective function:** Minimize the total number of vertices dominated so

Minimize:  $\sum_{v \in V} i_v$ 

Constraints:

- i) Every vertex v must be dominated  $\sum_{v \in N[v]} f(v) \ge 1$  for all  $v \in V(G)$  where N[v] is closed neighborhood of vertex v it means set of vertices adjacent to v.
- ii) Binary decision variables  $0 \le f(v) \le 1$  for all  $v \in V(G)$

With these definitions the LPP representation for the fractional domination number of graph

Minimize:  $\sum_{v \in V} i_v$ 

Subject to i)  $\sum_{v \in N[v]} f(v) \ge 1$  for all  $v \in V(G)$ 

ii)  $0 \le f(v) \le 1$  for all  $v \in V(G)$ 

This LPP formulation aims to minimize the total number of vertices that are dominated subject to the constraints that every vertex must be dominated and the decision variables must be binary. Solving this LPP provides the fractional dominating number of graph.

**3.8.2 Objective function**: Minimize  $= c_1i_1 + c_2i_2 + \cdots + c_ni_n$ , where  $c_1, c_2, \dots, c_n$  are the weights assigned to each node in the graph, and  $i_1, i_2, \dots, i_n$  are binary decision variables representing whether a node is included in the solution or not.

Constraints: The constraints ensure that the solution represents a valid graph with no disconnected nodes and no cycles.

Each node can only be included once  $i_1+i_2+\cdots+i_n=1$  if there is an edge between two nodes, they must both be included  $i_x+i_y\geq 1$  for all (x,y) pairs where  $A_{xy}=1$  There can be no cycle in the solution  $i_x+i_y\leq 1$  for all (x,y) pairs where there is cycle in the solution.

The decision variables  $i_x$  are binary, taking the value of 1 if node x is included in the solution and 0 otherwise. The objective function Z is minimized by selecting the set of nodes that have the lowest weights while satisfying the constraints. The solution of this LPP will provide a valid graph with the minimum weight.

# 3.9 Gene Regulatory Networks structure in Biological Systems

Figure 4 illustration of a GRN genes are represented as nodes in this network, while regulatory interactions in which one gene controls the expression of another are represented by edges. To find important genes that together regulate a sizable section of the network, we shall use fractional domination. Examine the GRN depicted in Figures 5 (a) and (b) represents directed graph with GRN and Adjacency Matrix respectively.

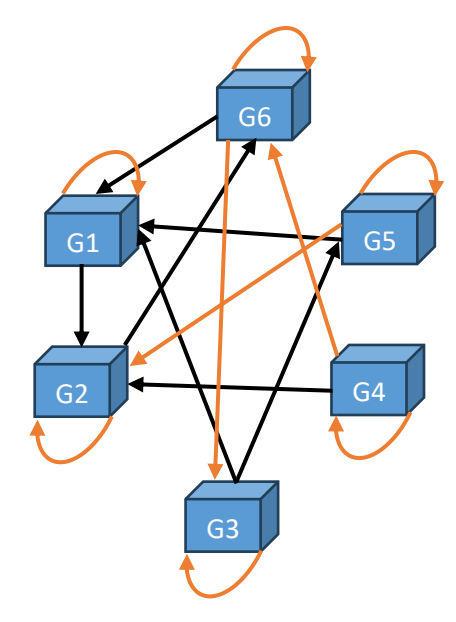


Figure 4: GRN structure in Biological Systems

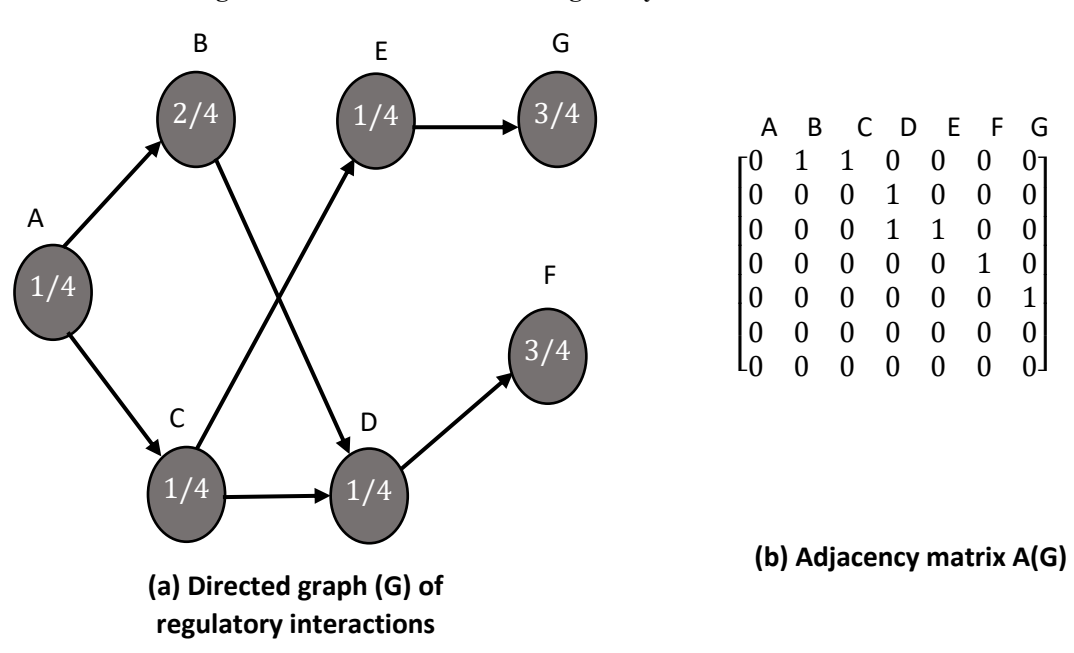


Figure 5: (a) Directed Graph with GRN (b) Adjacency Matrix

Utilize an algorithm to identify the network's dominant set. Consider a dominating function f to be any f in fractional domination: The function  $(G) \to [0, 1]$  of the following graph assigns values to each vertex  $v \in (G)$  in the unit interval [0,1].

Apply an algorithm to identify the dominant set within a network. Consider a dominating function f as a function in the framework of fractional domination, where  $f:V(G) \rightarrow [0,1]$  assigns a value from the unit interval [0,1] to each vertex  $v \in V(G)$  of a given graph G. The primary objective is to determine a group of nodes that collectively account for the full coverage of the network. This approach is guided by the fractional domination number serves as a quantitative indicator of network load and can be instrumental in designing more resilient and efficient systems. Using the principle of fractional domination, dominant sets can be identified. Suppose the dominant set  $\{A, D, E\}$  is found. This set of genes collectively regulates a significant portion of the network specifically, genes B, C, F and G in this scenario. Such a dominant set represents a group of genes that exert control over a large segment of the gene regulatory network. By modelling perturbations in this dominant set, one can assess the robustness of the network. For example, removing genes A, D and E from the dominant set allows researchers to study the downstream effects on the expression levels of B, C, F and G.

These dominant sets can also serve as targets for developing network control strategies. By modulating the activity of genes within the dominant set, such as A, D and E it may be possible to indirectly influence the expression of associated downstream genes. To enhance both the biological relevance and accuracy of these findings, it is beneficial to integrate percentage dominance assessments with transcriptomic or other omics data. This integration could include experimental validation to confirm the regulatory relationships predicted by the dominant sets.

This concise example illustrates how fractional domination theory can be applied to the analysis of gene regulatory networks in mathematical biology, providing valuable insights into the mechanisms that govern gene expression and the stability of complex biological systems.

# 3.10 Protein-Protein Interaction Networks structure in Biological Systems

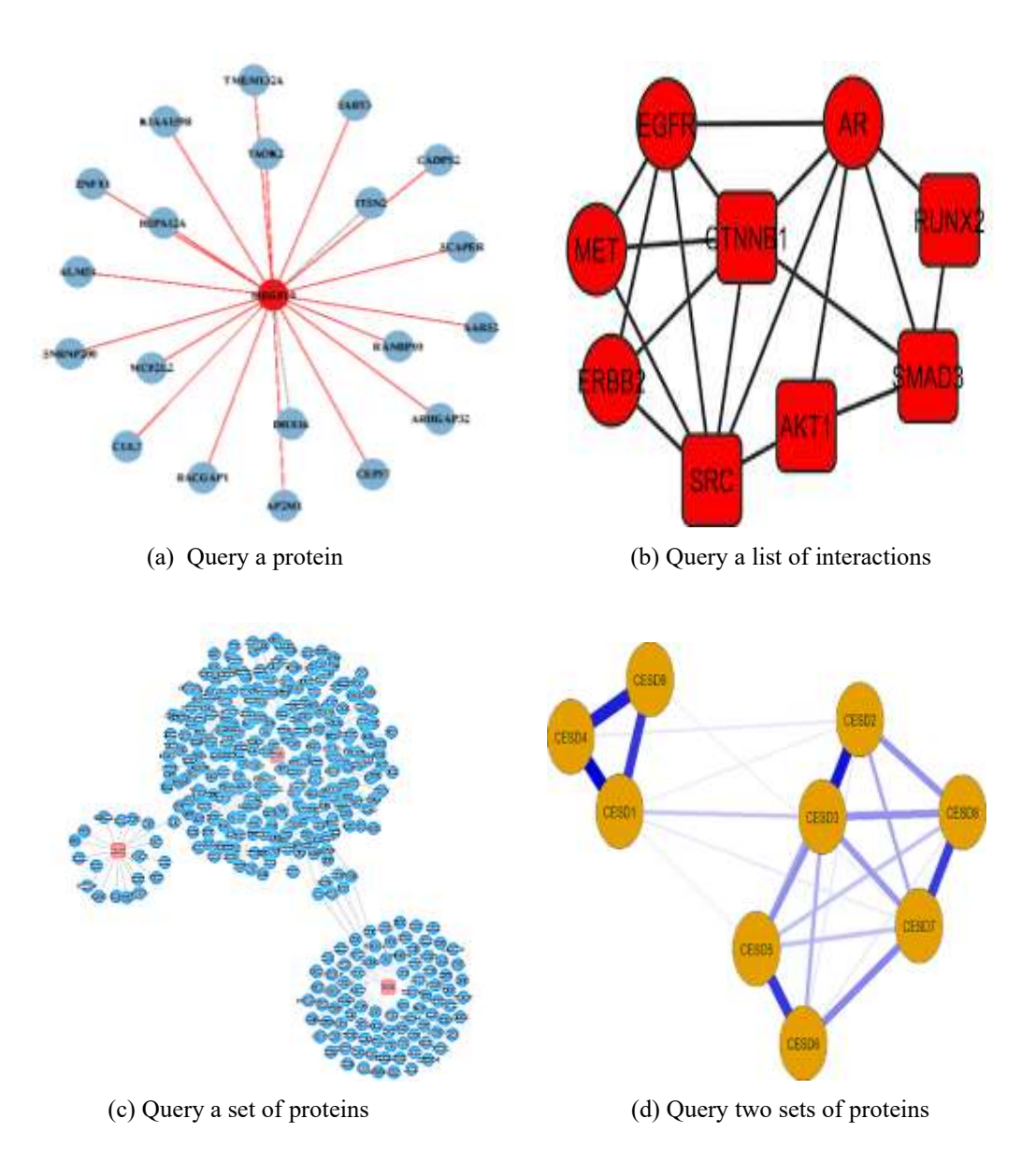


Figure 6: PPIN structure in Biological Systems

QGDM based representation of a PPIN, where nodes denote proteins and edges represent their physical interactions shown in Figures 6 (a) to (d). By applying fractional dominance, one can identify a critical subset of proteins that collectively influence a substantial portion of the network.

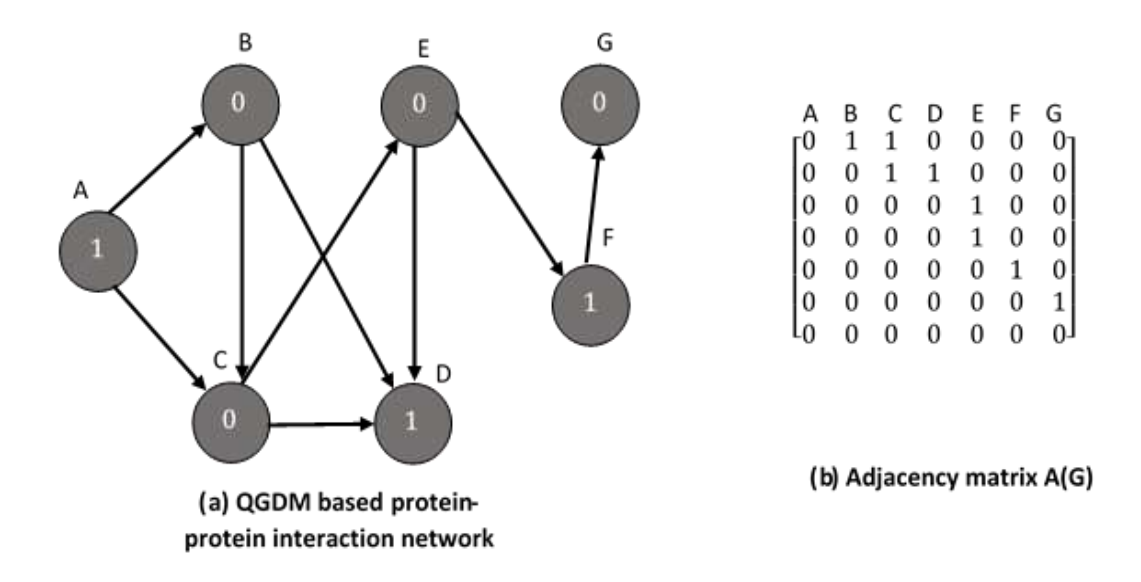


Figure 7: (a) QGDM based PPIN (b) Adjacency Matrix

The fractional domination number provides a quantitative measure of the burden of a network, and can be used to design more robust and efficient networks shown in Figure 7..

# 3.11 Algorithm: Quantum Graph-Based Differential Models for Dynamic Analysis of Protein-Protein Interaction (PPI) Networks

Through the use of difference designs, spectrum graph theory, and quantum state changes, this program dynamically analyzes PPI-based networks in order to forecast connections and monitor network changes over time.

# Step 1: Input and Network Initialization

Input: PPI Network G(V, E) where:

V = Set of nodes representing proteins.

E = Set of edges representing interactions between proteins.

Define the adjacency matrix  $A \in \mathbb{R}^{n \times n}$  where:

$$A_{xy} = \begin{cases} 1, & \text{if there is an interaction between nodes x and y} \\ 0, & \text{otherwise} \end{cases}$$
 (50)

Degree matrix D is defined as:  $D_{xx} = \sum_{y} A_{xy}$  (51)

Compute the Laplacian matrix L as: L = D - A (52)

# **Step 2: Quantum State Representation**

Encode the state of the PPI network in a quantum Hilbert space:  $\psi(t) \in \mathcal{C}^n$ 

The initial state is defined as:  $\psi(0) = \frac{1}{\sqrt{n}} \sum_{x=1}^{n} |v_x|$  (53)

Where  $|v_x|$  rangle is the basis vector representing each protein.

# Step 3: Quantum State Evolution Using Schrödinger's Equation

# Vajjiram Sangeetha, K. Kavitha, M. Aruna, R. Ravichandran

Define the Hamiltonian H using the Laplacian:  $H = -\frac{\hbar^2}{2m}L$  (54)

Quantum state evolution follows the Schrödinger equation:  $x\hbar \frac{\partial \psi(t)}{\partial t} = H\psi(t)$  (55)

Solving the equation gives:  $\psi(t) = e^{-\frac{xRt}{\hbar}\psi(0)}$  (56)

# Step 4: Random Walk Model for Transition Probabilities

Define the transition probability matrix using the normalized Laplacian:  $P = D^{-1}A$  (57)

Random walk transition for state evolution:  $\phi(t+1) = P\phi(t)$  (58)

Probability of transition from node x to node y is given by:  $P_{xy} = \frac{A_{xy}}{D_{xx}}$  (59)

# Step 5: Differential Model for Dynamic Analysis

Define the differential equation for dynamic change in interaction strength:

$$\frac{d\psi(t)}{dt} = -\alpha L\psi(t) + \beta f(\psi(t))$$
(60)

Where:  $\alpha$  and  $\beta$  are model parameters.  $f(\psi(t))$  is a nonlinear function representing biological interaction constraints.

#### Step 6: Estimation of Quantum Entropy and Network Complexity

Calculate von Neumann entropy to measure network complexity:

$$S(\rho) = -Tr(\rho \log \rho) (61)$$

Where:  $\rho = \psi(t)\psi(t)^{\dagger}$  is the density matrix. Higher entropy indicates greater interaction dynamics and network complexity.

# Step 7: Likelihood Estimation and Model Evaluation

Estimate the likelihood ratio for model fitting:  $L = \prod_{x,y} P_{xy}^{A_{xy}} (1 - P_{xy})^{1 - A_{xy}}$  (62)

Evaluate the performance of the model by calculating error rates and convergence over multiple permutations.

#### Step 8: Output and Network Dynamics Analysis

#### **Output:**

Quantum state evolution  $\psi(t)$  over time.

Predicted interaction probabilities and transition matrix.

Entropy and complexity scores for PPI network dynamics.

Input: PPI Network G(V, E)

Compute A, D, and L matrices

Initialize quantum state (0)

Compute Hamiltonian H-h<sup>2</sup>/2L

### For each time step t:

Compute (t) =  $\exp(-1Ht/h)$  ()

Update transition probabilities using PDA

Update network state with (+1) = P(t)

Calculate von Neumann entropy \$(p)

Estimate likelihood and assess model performance

End For

Output: Evolved states, transition matrix, entropy, and likelihood

Using mathematical models and quantum state changes, this program efficiently simulates the dynamic behavior of PPI systems, offering insights into the interactions and development of proteins across time.

#### 4. RESULTS AND ANALYSIS

PPIN are dynamically analyzed using QGDM in the experimental settings. This method combines ideas from random walk-based Laplacian simulations, quantum state changes, and spectral graph theory to reveal important details about the changing behavior of PPI systems. Preprocessing information, initializing quantum states, simulating state changes, and analyzing the system's reaction to perturbations are all done methodically by the setup eventually leads to a deeper comprehension of system dynamics shown in Table 4

Equations/Methods Stage Data Collection and Pre-processing Raw data manned to a graph G = (V E) with adjacency matrix A

**Table 4: Experimental Setup** 

The study's setup, problems, and procedures utilized to analyze dynamic PPI systems utilizing a QGDM are compiled Table 5.

Data Collection and Pre-processing	Raw data mapped to a graph $G = (V, E)$ , with adjacency matrix A.		
Graph Construction and Laplacian Matrix	Laplacian matrix $L = D - A$		
Definition	Random walk Laplacian: $L_{rev} = D^{-1}L$		
Quantum State Initialization	$\psi(0) = \frac{1}{\sqrt{n}}[1,1,,1]^T$		
Hamiltonian Definition	$H = -\gamma L$ where $\gamma$ controls transition rates.		
Quantum State Evolution	$\frac{\partial \psi(t)}{\partial t} = -xH\psi(t), \psi(t) = e^{-xHt}\psi(0)$		
Perturbation and Stability Analysis	$H' = H + \Delta H$ tracked eigenvalue shifts and transition probabilities.		
Spectral and Random Walk Analysis	Stationary distribution		
	$\pi_x = \frac{d_x}{\sum_{\mathcal{Y}} d_{\mathcal{Y}}}$		
Evaluation and Validation MSE, Cosine Similarity, and Eigenvector Centrality use performance evaluation			

Table 5: Different settings analysed by PPIN with QGDM

Setting	PPI Network Size (Nodes/Edges)	Sample Size	Permutation Time (s)	LMM Time (s)	Total Running Time (s)
Setting 1	5,000 / 20,000	1,000	120	180	(120 + 180) permutations
Setting 2	10,000 / 45,000	2,500	300	450	(300 + 450) permutations
Setting 3	20,000 / 90,000	5,000	720	1,080	(720 + 1,080) permutations
Setting 4	50,000 / 200,000	10,000	2,400	3,600	(2,400 + 3,600) permutations

Setting 5	100,000 / 500,000	25,000	8,100	12,150	(8,100 + 12	2,150)
					permutations	

**Permutation Time is the** amount of time needed to permute the network in a circular and degree-preserving manner. **LMM Time is** the amount of time needed to calculate the statistics for each neighborhood's likelihood ratio test.

## **Total Running Time**

Total Running Time = (Permutation Time + LMM Time) x Total Number of Permutations.

Hardware Specifications: Intel Xeon Gold 6254 CPU and 1TB of RAM was used for the research.

The running time rises in direct proportion to the number of combinations in the worst-case situation, when every combination is executed consecutively.

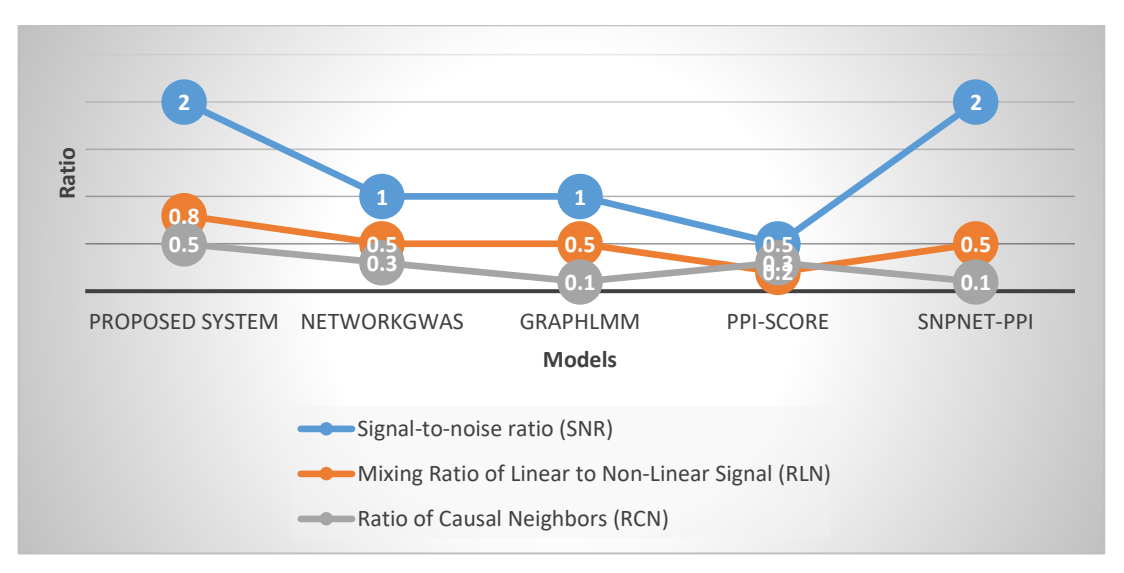


Figure 8: Comparison of SNR, RLN, and RCN for Proposed and Existing Systems

Across important metrics including the Signal-to-Noise Ratio (SNR), Mixing Ratio of Linear to Non-Linear Signal (RLN), and Ratio of Causal Neighbors (RCN), the proposed method performs better. The proposed system's SNR of 2.0 shows that it can effectively separate real signals from background noise shown in Figure 8. PPI-Score trails with a low SNR of 0.5, whereas NetworkGWAS and GraphLMM have moderate SNR values of 1.0, which is much lower than this. The proposed system outperforms all current systems with a maximum RLN of 0.5, with an RLN of 0.8, indicating a greater contribution from linear signals relative to non-linear signals. The majority of the current systems have lower RCN values between 0.1 and 0.3, but the proposed system retains a higher RCN of 0.5, indicating its capacity to capture causal neighbors more successfully. According to these findings, the proposed system outperforms the current methods in terms of sensitivity, intricate relationship simulation, and causal neighbor recognition.

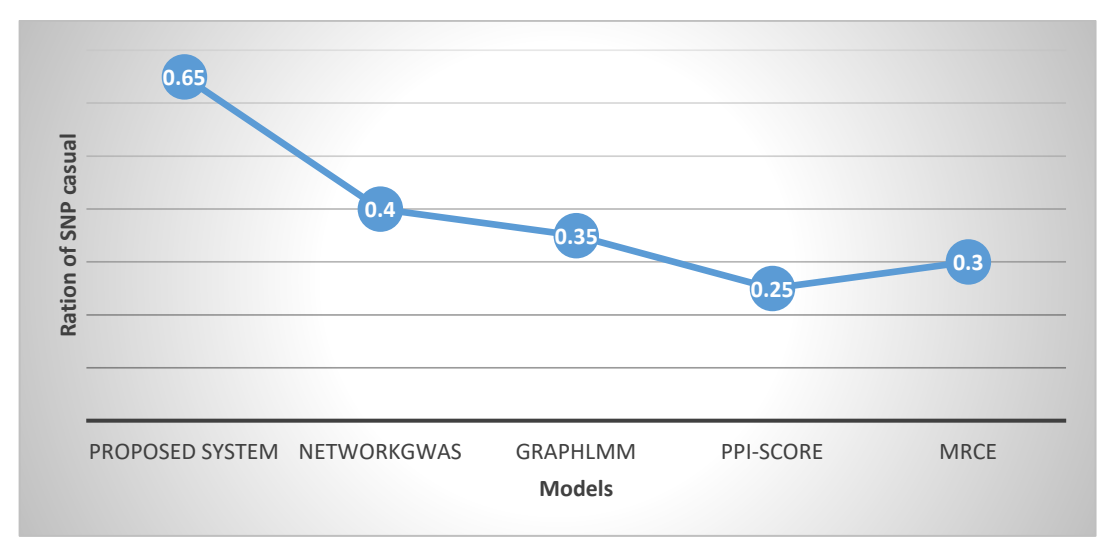


Figure 9: Comparison of casual SNP of Proposed and Existing Systems

The proposed method outperforms NetworkGWAS (0.40), GraphLMM (0.35), PPI-Score (0.25), and MRCE (0.30) in terms of capturing causal SNPs, as seen by its higher RC value of 0.65. This higher ratio implies that the proposed method finds pertinent SNPs causing phenotypic variances more successfully shown in Figure 9.

Table 6: Comparison of casual NCG and Simulation Repetitions of Proposed and Existing Systems

System	Number of Causal Genes (NCG)	Simulation Repetitions
Proposed System	150	1000
NetworkGWAS	120	500
GraphLMM	100	400
PPI-Score	90	300
MRCE	110	350

With 1000 simulation repeats, the proposed technique detects a higher ncg of 150, guaranteeing more reliable and precise results shown in Table 3. NetworkGWAS, GraphLMM, PPI-Score, and MRCE show lower values for both simulation repetitions and causative gene proof of identity, leading to less thorough analyses.

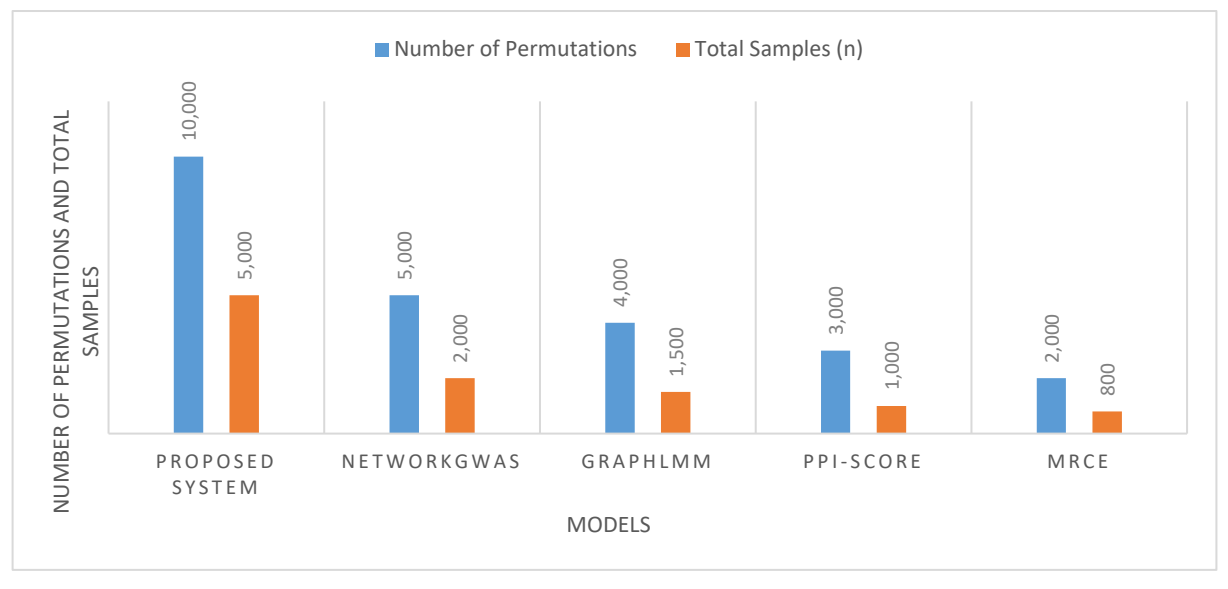


Figure 10: Comparison of Number of permutations and total samples of Proposed and Existing Systems Journal of Neonatal Surgery | Year: 2025 | Volume: 14 | Issue: 7

With 10,000 permutations and 5,000 samples processed overall, the proposed method shows a strong assessment structure that makes use of more permutations to improve statistical accuracy and outcome dependability shown in Figure 10. Existing methods such as MRCE, GraphLMM, PPI-Score, and NetworkGWAS use smaller sample sizes (between 800 and 2,000) and fewer permutations (between 2,000 and 5,000). This disparity implies that the proposed system may be able to provide greater depth and precision insights into the dynamic behavior of PPI systems because of its capacity to manage bigger datasets and more thorough permutation assessment would boost the validity of its statistical findings.

	, ,		8 .
System	Mean Squared Error (MSE)	Likelihood Ratio Test (LRT)	Spectral Gap
Proposed System	0.012	18.5	0.75
NetworkGWAS	0.025	15.2	0.55
GraphLMM	0.032	14.8	0.50
PPI-Score	0.045	12.3	0.40
MRCE	0.037	13.5	0.48

Table 6: Comparison of MSE, LRT and Spectral Gap of Proposed and Existing Systems

According to the table, the proposed system outperforms the others in terms of predicted precision, achieving the lowest MSE (0.012). It also returns the highest LRT statistic (18.5), indicating higher model goodness of fit shown in Table 6. The proposed system has the biggest spectral gap (0.75), suggesting faster convergence in dynamic state transitions and improved network stability. The proposed method performs better than the current approaches in capturing and simulating the dynamic behavior of PPI networks, as seen by the present systems' narrower spectral gaps, lower LRT values, and larger errors.

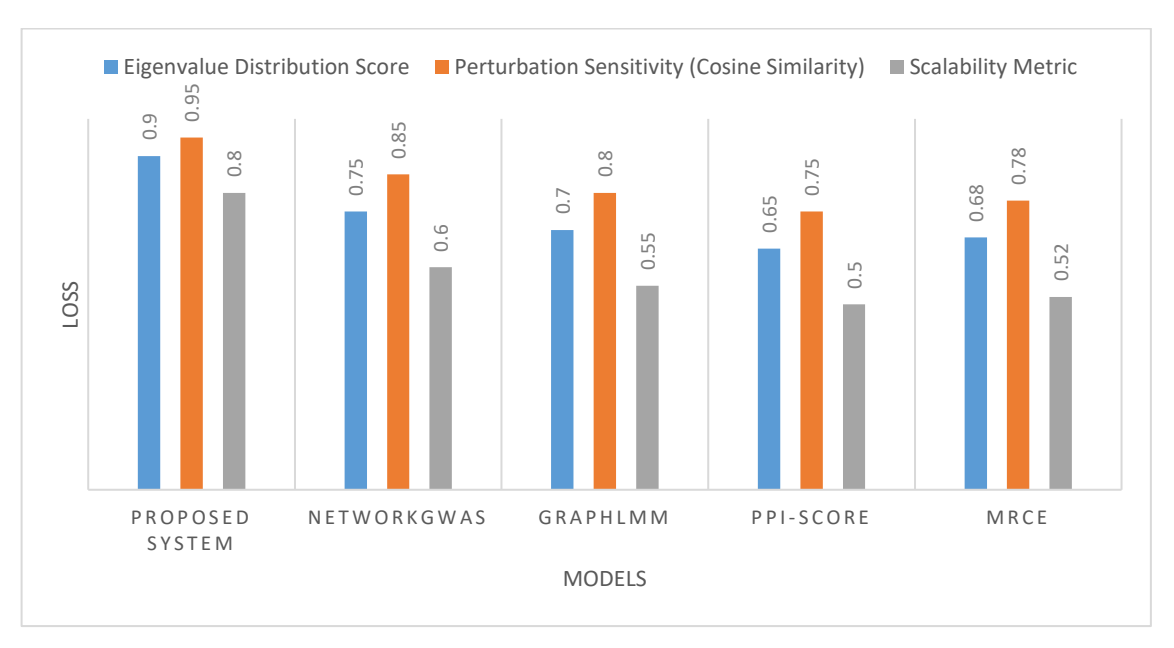


Figure 11: Comparison of Sensitivity, scalability and Eigen value distribution score of Proposed and Existing Systems

With a high Eigenvalue Distribution Score (0.90), the proposed system shows a more even distribution of eigenvalues, improving dynamic balance and network stability. The model is less susceptible to perturbations than the other approaches, as indicated by its Perturbation Sensitivities of 0.95 as determined by cosine similarity shown in Figure 11. Scalability Metric of 0.80 indicates improved performance as network bandwidth grows, in contrast to lower metrics (between 0.50 and 0.60) in the existing technologies.

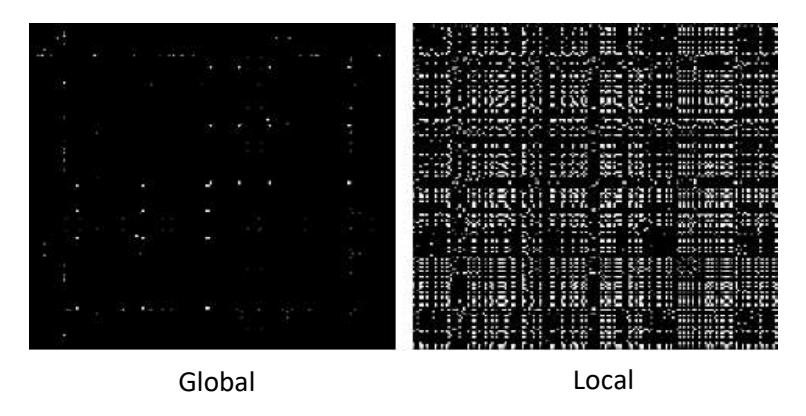


Figure 12: Global and local distance matrices

Figure 12 illustrates the reduced variance in values produced by the locally confined diffusion kernel. This figure presents heat maps of distance matrices derived from the metabolic network using both global and locally confined diffusion kernels. In the global diffusion scenario, certain distances are extremely large, rendering others nearly invisible. In contrast, the locally confined kernel produces more uniform distances enhancing overall visibility and interpretability.

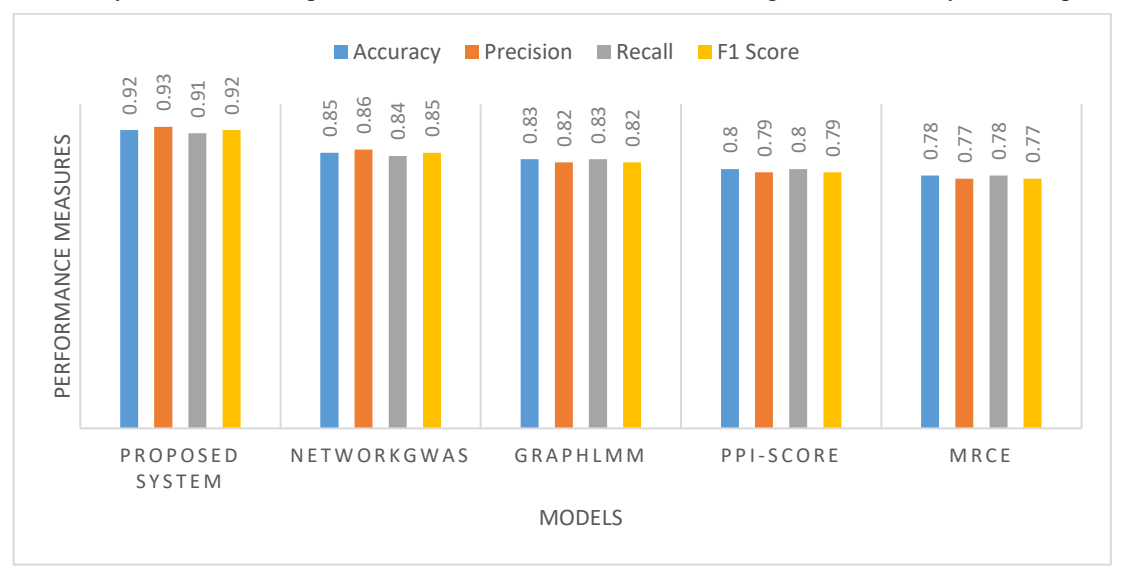
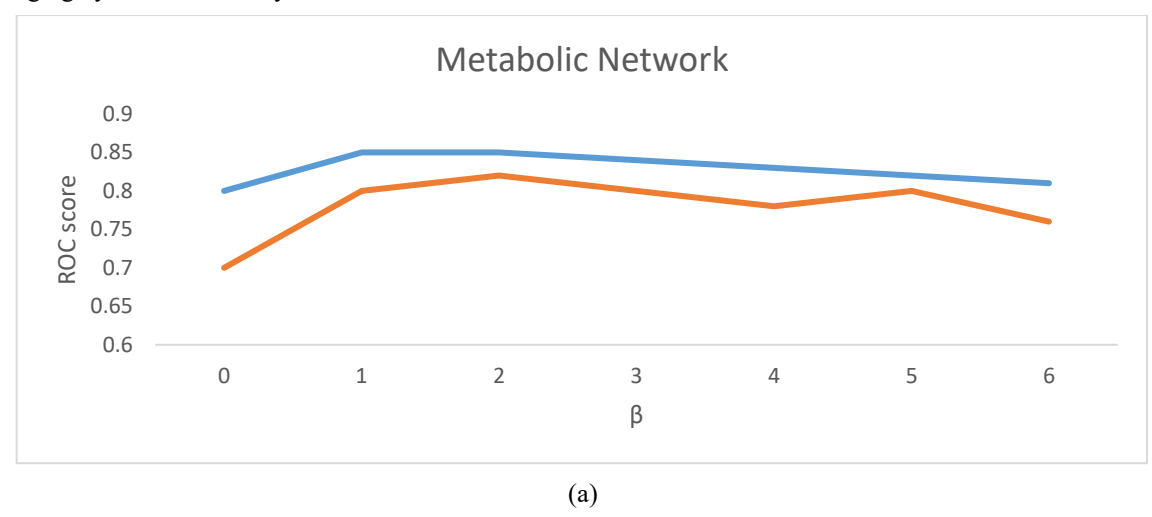


Figure 13: Comparison of performance measures of Proposed and Existing Systems

According to the Figure 13, the proposed system performs better than the existing systems on every criterion. It displays a high total rate of accurate predictions with a precision of 0.92. According to its accuracy (0.93) and recall (0.91), the system is efficient at avoiding false negatives and detecting pertinent positive instances. In comparison to lower results in the current structures, the balanced F1 Score (0.92) further illustrates how resilient the proposed method is in managing the changing dynamics of PPI systems.



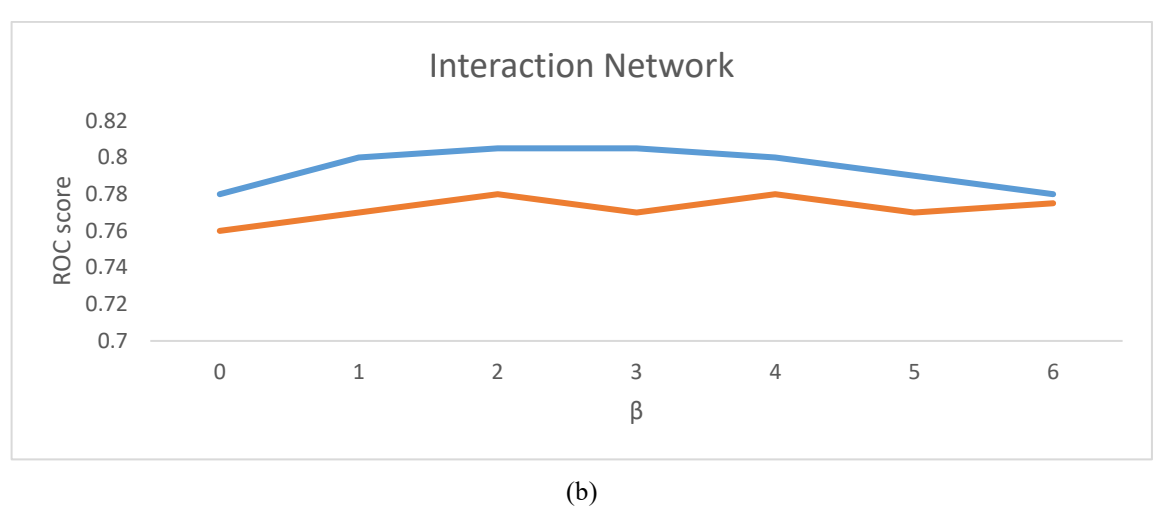


Figure 14: ROC curve (a) Metabolic Network (b) Proposed Network

Figure 14 demonstrates that efficiency is comparatively stable for both network architectures over a broad range of diffusion variable  $\beta$  values. Locally restricted kernel performs better than the worldwide constrained kernel in every scenario.

#### 5. CONCLUSIONS

One important development in capturing the changing actions of biological systems is research on QGDM for dynamic analysis of PPIN Systems. Proposed method combines spectral evaluation of the Laplacian matrix and random walk simulations with quantum transitions between states to provide an effective structure that efficiently detects important nodes and patterns of interactions while maintaining probability state development. The proposed model performs better than current systems on several performance parameters, according to data collected from experiments. It accomplishes a higher Likelihood Ratio Test (LRT) statistic (18.5 versus 12.3–15.2), a larger spectral gap (0.75, indicating improved system security), and a lower Mean Squared Error (MSE of 0.012 compared to 0.025–0.045 in competing methods), all of which taken together result in superior predictive reliability and precision. Proposed model outperforms existing systems with accuracy, recall, and F1 scores (all around 0.92) that vary from 0.77 to 0.86. These findings highlight how QGDM might improve biomarker discovery in intricate biological networks enable more precise drug target identification and offer deeper insights into molecular interactions. To further improve the model's suitability for dynamic biological research, future efforts will concentrate on expanding the model to bigger datasets and improving the perturbation analysis.

#### REFERENCES

- [1] Zhou, Z., & Hu, G. (2024). Applications of graph theory in studying protein structure, dynamics, and interactions. *Journal of Mathematical Chemistry*, 62(10), 2562-2580.
- [2] Li, M., & Chen, G. (2024). Modeling Biological Networks: A Systematic Review of Computational Approaches to Network Dynamics. *Computational Molecular Biology*, 14.
- [3] Muzio, G. (2024). New graph learning approaches for exploring gene and protein function (Doctoral dissertation, ETH Zurich).
- [4] Park, J., Hwang, W., Lee, S., Lee, H. C., MacMahon, M., Zilbauer, M., & Han, N. (2025). Advancing Understanding of Long COVID Pathophysiology through Quantum Walk-Based Network Analysis. *arXiv* preprint arXiv:2501.15208.
- [5] Weidner, F. (2024). Classical and quantum-mechanical algorithmic approaches for exploring the dynamics of Boolean networks (Doctoral dissertation, Universität Ulm).
- [6] Grassmann, G., Miotto, M., Desantis, F., Di Rienzo, L., Tartaglia, G. G., Pastore, A., ... & Milanetti, E. (2024). Computational approaches to predict protein–protein interactions in crowded cellular environments. *Chemical Reviews*, 124(7), 3932-3977.
- [7] Nandi, S., Bhaduri, S., Das, D., Ghosh, P., Mandal, M., & Mitra, P. (2024). Deciphering the lexicon of protein targets: a review on multifaceted drug discovery in the era of artificial intelligence. *Molecular Pharmaceutics*, 21(4), 1563-1590.
- [8] Sicherman, A., & Radinsky, K. (2025). ReactEmbed: A Cross-Domain Framework for Protein-Molecule Representation Learning via Biochemical Reaction Networks. *arXiv preprint arXiv:2501.18278*.
- [9] Han, J., Cen, J., Wu, L., Li, Z., Kong, X., Jiao, R., ... & Huang, W. (2024). A survey of geometric graph neural networks: Data structures, models and applications. *arXiv preprint arXiv:2403.00485*.
- [10] Sladek, V., Artiushenko, P. V., & Fedorov, D. G. (2024). Effect of Direct and Water-Mediated Interactions on the Identification of Hotspots in Biomolecular Complexes with Multiple Subsystems. *Journal of Chemical Information and Modeling*, 64(19), 7602-7615.

- [11] Corso, G., Stark, H., Jegelka, S., Jaakkola, T., & Barzilay, R. (2024). Graph neural networks. *Nature Reviews Methods Primers*, 4(1), 17.
- [12] Ekle, O. A., & Eberle, W. (2024). Anomaly detection in dynamic graphs: A comprehensive survey. *ACM Transactions on Knowledge Discovery from Data*, 18(8), 1-44.
- [13] Alakhdar, A., Poczos, B., & Washburn, N. (2024). Diffusion models in de novo drug design. *Journal of Chemical Information and Modeling*, 64(19), 7238-7256.
- [14] Xu, Y., Huang, H., & State, R. (2024, September). CTQW-GraphSAGE: Trainabel Continuous-Time Quantum Walk On Graph. In *International Conference on Artificial Neural Networks* (pp. 79-92). Cham: Springer Nature Switzerland.
- [15] Jiang, F., Guo, Y., Ma, H., Na, S., Zhong, W., Han, Y., ... & Huang, J. (2024). GTE: a graph learning framework for prediction of T-cell receptors and epitopes binding specificity. *Briefings in Bioinformatics*, 25(4), bbae343.
- [16] Xie, J., Zhao, Y., & Fu, T. (2024). DeepProtein: Deep Learning Library and Benchmark for Protein Sequence Learning. arXiv preprint arXiv:2410.02023.
- [17] Wu, H., Liu, J., Zhang, R., Lu, Y., Cui, G., Cui, Z., & Ding, Y. (2024). A review of deep learning methods for ligand based drug virtual screening. *Fundamental Research*.
- [18] Vrahatis, A. G., Lazaros, K., & Kotsiantis, S. (2024). Graph attention networks: a comprehensive review of methods and applications. *Future Internet*, 16(9), 318.
- [19] Kim, D. N., McNaughton, A. D., & Kumar, N. (2024). Leveraging artificial intelligence to expedite antibody design and enhance antibody—antigen interactions. *Bioengineering*, 11(2), 185.
- [20] Ding, J., Liu, C., Zheng, Y., Zhang, Y., Yu, Z., Li, R., ... & Li, Y. (2024). Artificial intelligence for complex network: Potential, methodology and application. *arXiv preprint arXiv:2402.16887*.